[RuII(tpy)(bpy)Cl]+-Catalyzed Reduction of Carbon Dioxide. Mechanistic Insights by Carbon-13 Kinetic Isotope Effects

Please do not adjust margins
ChemComm

Chemical Communications

COMMUNICATION

[Ru^{II}(tpy)(bpy)Cl]$^+$-Catalyzed Reduction of Carbon Dioxide. Mechanistic Insights by Carbon-13 Kinetic Isotope Effect

T. W. Schneider,[a] M. Hren,[a] M. Z. Ertem,*[b] and A. M. Angeles-Boza,*[a,c]

In this work, we examine the use of competitive ^{13}C kinetic isotope effects (^{13}C KIEs) on CO_2 reduction reactions that produce CO and formic acid as a means to formulate reaction mechanisms. The findings reported here mark a further advancement in the combined ^{13}C KIE measurements and theoretical calculations methodology for probing CO_2 conversion reactions.

Conversion of CO_2 into useful chemicals such as CO, formic acid, or methanol by activation/reduction is one of the most important and interesting topics of research given modern energy and environmental concerns.[1] Since the 1970s, when Aresta and Nobile synthesized and crystallographically characterized several metal complexes containing CO_2,[2-4] a number of catalytic systems capable of performing the activation of CO_2 have been explored.[5-7] These early results, combined with the fact that metal complexes are among the most effective catalysts for many chemical reactions, has led to extensive research effort toward developing metal-based CO_2 activation systems. Understanding the formation and properties of activated metal–CO_2 complexes will not only unravel the basis of their complex reactivities but will also guide further synthetic modifications for the development of metal-based catalysts that are more efficient, inexpensive and environmentally friendly.

A variety of experimental tools and computational methods have been applied to study CO_2 activation; however, fast reaction rates and elusive reaction intermediates have made it difficult to establish rate-determining steps (rds) and probe catalytic mechanisms. Heavy atom isotope effects is a technique that, historically, has been routinely used to afford insight into the nature of the transition state for the rds in enzyme catalysis.[8-10] However, in recent years, competitive

KIEs at natural abundance levels have been used to probe the mechanisms of small molecule activation by transition metal complexes during turnover conditions.[11-15] The information gained from natural abundance KIEs measurements is especially powerful when coupled with theoretical calculations. For example, ^{18}O KIE determinations have been used to formulate mechanisms of O-O bond formation.[11-14] We recently expanded the scope of this technique by probing the mechanism of the photocatalytic CO_2 reduction by the well-known Lehn's catalyst, Re(bpy)(CO)$_3$Cl (bpy = 2,2'-bipyridine).[15] We now focus on using ^{13}C KIEs in reactions in which more than one product is formed, a very common outcome among CO_2 reduction catalysts.

As a proof-of-concept, we sought to study a system capable of producing two distinct products using a robust metal catalyst. A perusal of the literature indicated that the catalyst precursor [Ru^{II}(tpy)(bpy)Cl]$^+$ (**1**, tpy = 2,2':6',2"-
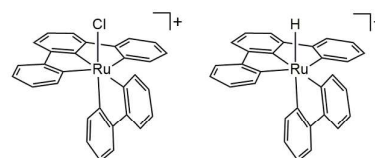
Fig. 1 Schematic representations of [Ru^{II}(tpy)(bpy)Cl]$^+$ **(1)** and [Ru^{II}(tpy)(bpy)H]$^+$ **(2)**

terpyridine) is the ideal model as **1** and its derivatives have been shown to produce CO in electrochemical reductive processes,[16-18] and it is very likely that **1** can reduce CO_2 under photochemical conditions in the presence of a sacrificial electron donor similarly to other ruthenium(II) photocatalysts.[5] In addition, the hydride derivative of **1**, [Ru^{II}(tpy)(bpy)H]$^+$ **(2)** can produce formate upon CO_2 insertion into the Ru-H bond.[19-22] Moreover, Matsubara *et al.* demonstrated that **2** can be formed by irradiation of [Ru^{II}(tpy)(bpy)(DMF)]$^+$ (DMF = N,N-dimethylformamide) in the presence of triethylamine with moderate yields.[23] Therefore, we hypothesized that a solution of **1** in the presence of triethanolamine (TEOA) and CO_2 will produce both CO and formate.

[a.] *Department of Chemistry, University of Connecticut, Storrs, CT 06269, USA*
[b.] *Chemistry Division, Energy & Photon Sciences Directorate, Brookhaven National Laboratory, Building 555A, Upton, New York 11973, USA*
[c.] *Institute of Materials Science, University of Connecticut, Storrs, CT 06269, USA*
† Footnotes relating to the title and/or authors should appear here.
Electronic Supplementary Information (ESI) available: [details of any supplementary information available should be included here]. See DOI: 10.1039/x0xx00000x

Please do not adjust margins

Photochemical formation of CO and formate. In a typical run, a solution of **1** in a 5:1 acetonitrile/TEOA solvent mixture containing 1 equivalent of $[Ru(bpy)_3]Cl_2$ (RuTB), and saturated with 100% CO_2 was irradiated under visible light. RuTB is a photosensitizer with an outer sphere electron transfer rate near that of the diffusion limit.[24] We observed that this photosensitizer was needed for **1** to exhibit catalytic behavior under the reaction conditions. The irradiation times ranged from 2 to 24 hours. Formation of CO was determined using gas chromatography (GC) (Figure S1). As hypothesized, we observed the formation of formate which was quantified by ^{1}H-NMR, using a method involving Verkade's Base, as was recently described by Kubiak and coworkers (Figures S2 and S3).[25] The yields for both CO and formic acid were calculated and are presented in Figure 2a in terms of turnover number (TON). Experiments were also ran in the presence of 1% H_2O (Figure S4).

Experimental Kinetic Isotope Effect. The ^{13}C KIEs for CO_2 reduction were determined using a previously established competitive methodology.[15,26] CO_2 reduction under photocatalytic conditions involved a solvent mixture that was 5:1 acetonitrile/TEOA. An additional set of experiments contained 1% H_2O in a 5:1 acetonitrile/TEOA solution. The solutions were saturated with a gas mixture that was 3% CO_2 in N_2. This mixture was then injected into a reaction vessel containing equimolar amounts of **1** and RuTB. The reaction mixture was irradiated under a visible light source ($\lambda \geq 400$ nm, 1000 V FEL bulb with band-pass filter) while stirring. After catalysis had been performed, the remaining CO_2 was isolated. The isolation process involved a series of cold traps designed to separate the CO_2 from such impurities as N_2, CO, or solvent vapor. The pressure of the remaining CO_2 was measured with a digital manometer, and then frozen and sealed into a glass

Fig. 2 (A) CO (red circles) and formic acid (blue triangles) are formed during the photocatalytic reduction of CO_2 catalyzed by **1**. Data points are shown with error bars representing standard deviations from two measurements each. (B) Isotope fractionation of CO_2 during its reduction catalysed by **1**. Data points are shown with error bars representing standard errors.

ampule. The isotope ratio of each CO_2 sample was measured with an isotope ratio mass spectrometer (IR-MS).

Figure 2b shows the plot of $\ln(R_f/R_0)$ vs $\ln(1-f)$ for CO_2 reduction by the catalytic system, in which f is the fraction of CO_2 which has been catalytically reduced, and R_0 and R_f are the ^{12}C/^{13}C isotope ratios of CO_2 before and after fractionation, respectively. Using equation 1, we determined that the

reactions under "dry" conditions and with 1% added water resulted in ^{13}C KIE values of 1.052 ± 0.004 and 1.044 ± 0.006, respectively.

$$\ln\left(\frac{R_f}{R_0}\right) = \left(1 - \frac{1}{KIE}\right)\ln(1-f) \qquad (1)$$

Theoretical Investigation of the Photocatalytic Reduction of CO_2 by 1. Density Functional Theory (DFT) calculations at the M06 level of theory[27] with the SMD continuum solvation model[28] were performed to investigate the photocatalytic CO_2 reduction mechanism by **1**, and to compute the corresponding ^{13}C isotope effects of the optimized structures in the catalytic cycle. The proposed catalytic cycle and the computed free energy changes (ΔG) for the reduction of CO_2 by **1** under catalytic conditions are presented in Scheme 1. Optimized structures are in Table S1 in the Supporting Information. The various branching pathways which could lead to potential side products are shown in Scheme S1.

The proposed mechanism for the reduction of CO_2 to CO starts with a pair of one-electron reductions, the first with a potential of -1.51 V, and the second with a potential of -1.99 V vs SCE (Scheme 1). The second reduction leads to the dissociation of chloride ion with an activation free energy ($\Delta G^\ddagger$) of 5.4 kcal/mol, and a free energy change (ΔG) of -7.5 kcal/mol, generating the neutral two-electron reduced **[Ru]**[0]. The binding of CO_2 molecule to **[Ru]**[0] proceeds with $\Delta G^\ddagger = 9.3$ kcal/mol and this process involves net two electron transfer from the complex to CO_2,[16] resulting in the formation of **[Ru–CO$_2$]**[0]. We also considered the possibility of the chloro ligand dissociating from the one-electron reduced **[Ru–Cl]**[0] species, and the subsequent binding of CO_2 to the **[Ru]**[+] but the calculated $\Delta G^\ddagger$s were significantly higher than those steps involving their two-electron reduced counterparts, and their products were much less stable (Scheme S1). The generated **[Ru–CO$_2$]**[0] can follow two reactions pathways. The first one is the addition of a second CO_2 molecule to the complex, which would result in the formation of one equivalent of CO and CO_3^{2-} ($\Delta G^\ddagger = 24.1$ kcal/mol). The second possible pathway is the protonation of **[Ru–CO$_2$]**[0] forming **[Ru–C(O)OH]**[+]. This process is barrierless, and has ΔG of -20.9 kcal/mol (Scheme 1). Due to the fact that the addition of a proton both has lower activation energy requirements and results in a more stable product, we are confident that this protonation step is the more likely of the two.

[Ru–C(O)OH][+] can then either **(i)** react with another CO_2 molecule, leading to the production of CO and HCO_3^- ($\Delta G^\ddagger = 28.6$ kcal/mol) or **(ii)** react with a proton donor with concomitant cleavage of C—OH to generate **[Ru–CO]**[+] and a water molecule ($\Delta G^\ddagger = 16.3$ and 24.1 kcal/mol respectively for TEOAH[+] and H_2O as the proton source) or **(iii)** alternatively further reduced to generate **[Ru–C(O)OH]**[0]. Depending on the reaction conditions (*e.g.,* the pK_a of proton source) a competition between pathways **(ii)** and **(iii)** is predicted to exist whereas the $\Delta G^\ddagger$ associated with **(i)** is prohibitively high for this reaction route to be relevant.

Similarly to **[Ru–C(O)OH]$^+$**, **[Ru–C(O)OH]^0** can react with a CO_2 molecule to generate CO and HCO_3^- ($\Delta G^\ddagger$ = 24.0 kcal/mol), or C—OH bond cleavage could occur assisted via either TEOAH$^+$ ($\Delta G^\ddagger$ = 9.7 kcal/mol) or H_2O ($\Delta G^\ddagger$ = 17.4 kcal/mol) as the proton source. Again, C—OH bond breakage facilitated by TEOAH$^+$ is the most likely step based on computed activation free energies. The final common product **[Ru—CO]$^+$** for all different pathways is thought to evolve CO via further reduction reactions regenerating the reactive **[Ru]^0** species (Scheme 1).

In addition to the reduction of CO_2 to CO, production of formic acid was also observed in our experiments and the proposed catalytic cycle for the production of formic acid is presented in Scheme 1. The proposed mechanism starts with the protonation of vacant site on ruthenium center of **[Ru]^0** by TEOAH$^+$ ($\Delta G^\ddagger$ = 5.1 kcal/mol) to generate **[Ru–H]$^+$** species. This step is highly exergonic (ΔG = −28.3 kcal/mol) and computed pK_a for **[Ru]^0** is 31.2. The second step involves an electrophilic attack by CO_2 to **[Ru–H]$^+$** ($\Delta G^\ddagger$ = 13.2 kcal/mol) to form **[Ru–OCHO]$^+$** (ΔG = −0.2 kcal/mol), which represents the rate limiting step for the formate production pathway. Subsequent reduction steps will release formate and result in the formation of the reactive **[Ru]^0** species (Scheme 1).

The competition between protonation versus binding of CO_2 to **[Ru]^0** species will determine the product selectivity of **1** towards generation of formic acid and CO respectively. The computed $\Delta G^\ddagger$s are close for the protonation ($\Delta G^\ddagger$ = 5.1 kcal/mol) and CO_2 binding ($\Delta G^\ddagger$ = 9.3 kcal/mol) steps favoring the former pathway. Moreover, the relative concentration of the proton source and CO_2 as well as the pK_a of the proton source will impose a significant influence on relative production yields of formic acid and CO. Under the current experimental conditions, the yields of formic acid are larger than the yields of CO.

Interpretation of the competitive carbon-13 kinetic isotope effect. The experimentally observed ^{13}C KIE represents a weighted average of the ^{13}C KIEs for different pathways of CO_2 reduction leading to the formation of CO and formic acid as represented in equation 2,[30] where x is the fraction of CO_2 that was reduced to CO and (1-x) is the fraction reduced to formic acid.

$$KIE_{obs} = x\, KIE_{formic\ acid} + (1 - x)KIE_{CO} \qquad (2)$$

The fraction of formic acid under the employed reaction conditions is approximately 80% (Table S2).

Natural abundance level competitive KIEs include the isotope effects in mechanistic steps up to first irreversible step in catalytic reactions during turnover conditions. The proposed catalytic cycles indicate that for formic acid generation via the electrophilic attack of CO_2 to **[Ru–H]$^+$** is the first irreversible step whereas CO_2 binding to **[Ru]^0** species is the first irreversible step for the CO evolution pathway. The computed ^{13}C KIEs are $KIE_{formic\ acid}$ = 1.055 and KIE_{CO} = 1.068 for the above-mentioned steps. The weighted average according to equation 2 is KIE_{calc} = 1.058 which is in good agreement with the experimentally observed value of KIE_{expt} = 1.052 ± 0.004 and 1.044 ± 0.006. We also computed ^{13}C KIEs for several optimized transition state structures associated with different pathways and alternative assumptions for the first irreversible step for CO evolution pathway which are presented in the supporting information. Interestingly, the ^{13}C KIE for the CO pathway resembles the values found for the photochemical CO_2 reduction catalyzed by Re(bpy)(CO)$_3$Cl (~1.07) determined under similar conditions to those used in the current study.[15]

Within the context of Transition State Theory, the calculated KIEs can be further analyzed to provide insights into the contributions to the isotopic discrimination by the various terms, namely, $^{13}v_{RC}$ and $^{13}K_{TS}$ ($^{13}K_{TS}$ = ZPE × EXC × VP).[15,30] The computed isotope effects and individual terms indicate that for both the CO_2-binding (CO pathway) and CO_2 addition to **2** (HCO$_2$H pathway) $^{13}v_{RC}$ represents half of the ^{13}C KIEs observed
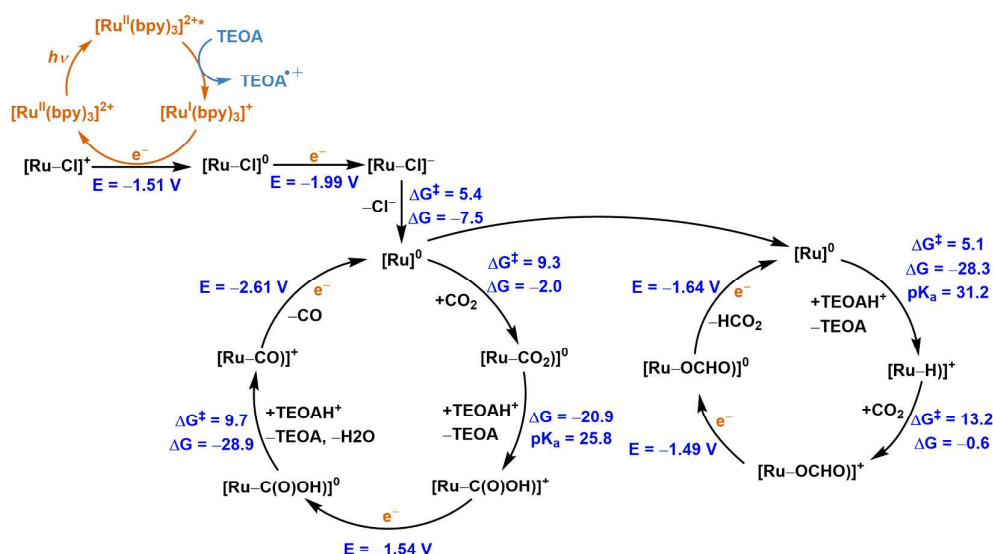
Scheme 1. Proposed reaction mechanism for CO and formate/formic acid generation from photocatalytic reduction of CO_2 starting for complex **1**. The computed free energy changes (ΔG) and activation free energies ($\Delta G^\ddagger$) are in units of kcal/mol and reduction potentials are reported vs SCE. See computational methods for details.

($^{13}v_{RC} \approx 1.03$) and large ZPE terms are responsible for the magnitude of the pseudoequilibrium constant ($^{13}K_{TS}$) values, 1.038 and 1.026 for the CO pathway and HCO_2H pathway, respectively. Remarkably, slightly larger $^{13}K_{TS}$ values, *c.a.* 1.05, were calculated for CO_2 binding by the one-electron and two-electron reduced species generated from Re(bpy)(CO)$_3$Cl also originating from a large contribution from the ZPE term.

In summary, we demonstrated that ^{13}C KIEs in combination with theoretical calculations can be used to study CO_2 reduction reactions in which two products are formed, and more importantly, we showed the detailed analysis of the determined values. We found that the first irreversible step in the CO pathway involves substrate binding to **1**. In the HCO_2H pathway, the results produced a large normal ^{13}C KIE for CO_2 insertion into the Ru-H bond with a more reactant-like transition state structure. This study serves as a reference point for mechanisms associated with Ru-catalyzed CO_2 transformations and demonstrates that ^{13}C KIEs coupled with theoretical calculations is a powerful method to investigate the mechanism of CO_2 reduction reactions.

Conflicts of interest

There are no conflicts to declare.

Notes and references

1. A. M. Appel, J. E. Bercaw, A. B. Bocarsly, H. Dobbek, D. L. DuBois, M. Dupuis, J. G. Ferry, E. Fujita, R. Hille, P. J. Kenis, C. A. Kerfeld, R. H. Morris, C. H. Peden, A. R. Portis, S. W. Ragsdale, T. B. Rauchfuss, J. N. Reek, L. C. Seefeldt, R. K. Thauer and G. L. Waldrop, *Chem. Rev.*, 2013, **113**, 6621-6658.
2. M. Aresta, C. F. Nobile, V. G. Albano, E. Forni and M. Manassero, *J. Chem. Soc., Chem. Commun.*, 1975, 636-637.
3. M. Aresta and C. F. Nobile, *J. Chem. Soc., Dalton Trans.*, 1977, 708-711.
4. M. Aresta, E. Quaranta and A. Ciccarese, *C1 Mol. Chem.*, 1985, **1**, 267-281.
5. Y. Tamaki, O. Ishitani, *ACS Catal.*, 2017, **7**, 3394-3409.
6. N. Elgrishi, M. B. Chambers, X. Wang, M. Fontecave, *Chem. Soc. Rev..*, 2017, **46**, 761-796.
7. K. A. Grice and C. P. Kubiak, *Adv. Inorg. Chem.*, 2014, **66**, 163-188.
8. A. C. Reyes, T. L. Amyes and J. P. Richard, *J. Am. Chem. Soc.*, 2016, **138**, 14526-14529.
9. P. Fristrup and N. Christensen, *Synlett*, 2015, **26**, 508-513.
10. M. W. Ruszczycky and V. E. Anderson, *J Theor Biol*, 2006, **243**, 328-342.
11. A. M. Angeles-Boza, M. Z. Ertem, R. Sarma, C. H. Ibañez, S. Maji, A. Llobet, C. J. Cramer and J. P. Roth, *Chem. Sci.*, 2014, **5**, 1141-1152.
12. R. Sarma, A. M. Angeles-Boza, D. W. Brinkley and J. P. Roth, *J. Am. Chem. Soc.*, 2012, **134**, 15371-15386.
13. A. M. Angeles-Boza and J. P. Roth, *Inorg. Chem.*, 2012, **51**, 4722-4729.
14. Khan, S.; Yang, K. R.; Ertem, M. Z.; Batista, V. S.; Brudvig, G. W. *ACS Catal*. 2015, **5**, 7104–7113.
15. T. W. Schneider, M. Z. Ertem, J. T. Muckerman and A. M. Angeles-Boza, *ACS Catalysis*, 2016, **6**, 5473-5481.
16. Z. Chen, C. Chen, D. R. Weinberg, P. Kang, J. J. Concepcion, D. P. Harrison, M. S. Brookhart and T. J. Meyer, *Chem. Commun.*, 2011, **47**, 12607-12609.
17. T. A. White, S. Maji and S. Ott, *Dalton Transactions*, 2014, **43**, 15028-15037.
18. B. A. Johnson, S. Maji, H. Agarwala, T. A. White, E. Mijangos and S. Ott, *Angew. Chem. Int. Ed.*, 2016, **55**, 1825-1829.
19. H. Konno, A. Kobayashi, K. Sakamoto, F. Fagalde, N. E. Katz, H. Saitoh and O. Ishitani, *Inorg. Chim. Acta*, 2000, **299**, 155-163.
20. Y. Matsubara, E. Fujita, M. D. Doherty, J. T. Muckerman and C. Creutz, *J. Am. Chem. Soc.*, 2012, **134**, 15743-15757.
21. J. R. Pugh, M. R. M. Bruce, B. P. Sullivan and T. J. Meyer, *Inorg. Chem.*, 1991, **30**, 86-91.
22. S. Kern and R. van Eldik, *Inorg. Chem.*, 2012, **51**, 7340-7345.
23. Y. Matsubara, H. Konno, A. Kobayashi and O. Ishitani, *Inorg. Chem.*, 2009, **48**, 10138-10145.
24. R. C. Young, R. Keene and T. J. Meyer, *J. Am. Chem. Soc.*, 1977, **99**, 2468-2473.
25. P. L. Cheung, C. W. Machan, A. Y. Malkhasian, J. Agarwal and C. P. Kubiak, *Inorg. Chem.*, 2016, **55**, 3192-3198.
26. T. W. Schneider and A. M. Angeles-Boza, *Dalton Trans*, 2015, **44**, 8784-8787.
27. Y. Zhao, D. G. Truhlar, *Acc. Chem. Res.* 2008, **41**, 157-167.
28. A. V. Marenich, C. J. Cramer, D. G. Truhlar, *J. Phys. Chem. B* 2009, **113**, 6378-6396.
29. K. Kalyanasundaram, *J. Chem. Soc., Faraday Trans. 2*, 1986, **82**, 2401-2415.
30. L. C. S. Melander and W. H. Saunders, *Reaction rates of isotopic molecules*, Wiley, 1980.

^{13}C kinetic isotope effect determinations combined with DFT calculations provide insight on the CO_2 reduction reaction catalyzed by a ruthenium complex.